Optik - International Journal for Light and Electron Optics 291 (2023) 171384

Contents lists available at ScienceDirect

Optik - International Journal for Light and Electron Optics

journal homepage: www.elsevier.com/locate/ijleo

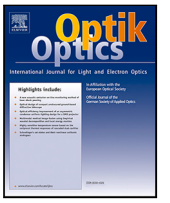

Original Research Article

Harnessing optical vortices to control current flow via quantized torque in coherently prepared multilevel atoms

Hamid R. Hamedi [a,*], Emmanuel Paspalakis [b]

[a] Institute of Theoretical Physics and Astronomy, Vilnius University, Saulėtekio 3, Vilnius LT 10257, Lithuania
[b] Materials Science Department, School of Natural Sciences, University of Patras, Patras 265 04, Greece

ARTICLE INFO

Keywords:
Light induced torque
Coherently prepared media
Optical vortices

ABSTRACT

This study delves into the interaction between coherently prepared trapped atoms and optical vortices, focusing on the intriguing phenomenon of light-induced torque enhancement and the resultant persistent current flow. Beginning with a three-level atom ensemble in the Λ configuration, we initiate a coherent superposition of lower levels to establish a coherent population trapping medium. The atoms interact with a pair of optical vortices, producing a quantized torque on each trapped atom that is directly proportional to the topological charge of the inhomogeneous coupling beams. This torque imparts a rotation to the entire ensemble, thereby generating a striking ring-shaped atomic current flow. With careful manipulation of the initial internal state of the atoms and the strength of the vortex pair, we can control the magnitude of the torque. Extending the model to include more complex level schemes with additional laser beams offers even greater potential for enhancing light-induced torque and refining our control over the current flow.

1. Introduction

The captivating interplay between laser pulses and atoms has shed light on a myriad of interesting phenomena, unveiling a rich landscape of optical marvels. Among these, we encounter the extensively explored effect of electromagnetically induced transparency (EIT) [1–6], where the interaction between light and matter unveils intriguing insights. Similarly, the stimulated Raman adiabatic passage (STIRAP) [7–9] beckons us with its alluring properties, while lasing without inversion (LWI) [10,11] captivates our attention with its unconventional characteristics. The domain of coherent population trapping (CPT) [12–15] stands as yet another inspiring phenomenon, where light–matter interactions lead to remarkable effects. This vast array of coherent optical phenomena finds practical applications in diverse areas, including the realm of slow light [3,4,16–18], where the control of light propagation velocity finds significant utility. Enhanced nonlinear optics [19–22] represents another frontier enriched by these phenomena, where the manipulation of light–matter interactions enables the enhancement of nonlinear optical effects. Furthermore, the storage of quantum information [23] and optical switching [24,25] emerge as promising applications stemming from these fascinating optical phenomena.

In the realm of light manipulation, the introduction of light beams with spiral phase dislocations has unfurled entirely new consequences. These beams, characterized by their phase cross-section and referred to as spiral phase $e^{il\phi}$, bear an orbital angular momentum (OAM) intricately tied to their azimuthal angle ϕ. A distinctive trait of these beams lies in the null field they create at their center, thanks to the spiral phase proportional to the azimuthal angle. The integer parameter l, also known as the topological

* Corresponding author.
E-mail addresses: hamid.hamedi@tfai.vu.lt (H.R. Hamedi), paspalak@upatras.gr (E. Paspalakis).

https://doi.org/10.1016/j.ijleo.2023.171384
Received 8 July 2023; Received in revised form 9 August 2023; Accepted 10 August 2023
Available online 13 September 2023

charge or order of the beam, represents the number of times the beam undergoes azimuthal 2π phase shifts [26,27]. This phase singularity situated at the beam's center bestows upon it a unique ring-shaped intensity profile, setting it apart from conventional light beams. The generation and manipulation of optical vortices housing phase singularities enable us to harness specific values of OAM [28–30], opening up exciting possibilities for optical exploration.

Optical vortices, renowned for their remarkable ability to carry orbital angular momentum, have unveiled a plethora of captivating phenomena when interacting with matter [31–40]. These effects have attracted substantial attention, especially concerning the influence of OAM on particles and atoms in a mechanical sense [41]. An exemplary instance is the utilization of light beams carrying OAM to induce rotational motion in particles confined by optical tweezers [42,43]. Moreover, the transfer of OAM to matter has been demonstrated to generate torque, thereby facilitating the transfer of wave energy [44–47].

Recent investigations have showcased the coherent transfer of photon OAM to a Bose–Einstein condensate (BEC) consisting of sodium atoms. This was achieved through a two-photon stimulated Raman process utilizing Laguerre–Gaussian (LG) beams [45]. By employing counterpropagating LG and Gaussian laser beams with matching linear polarization, the trapped atoms were subjected to axial confinement while simultaneously inducing an atomic vortex state by exerting torque on each atom's center of mass. Alternatively, Lembessis and Babiker proposed a distinct scenario for light-induced torque in a three-level Λ BEC of atoms. In this case, the BEC interacted with two counterpropagating vortex beams, resulting in the generation of a current flow [48]. The authors derived an expression for the induced torque acting on individual atoms, which ultimately led to a collective rotational effect on the entire BEC due to the approximation of its many-body wave function as the product of identical single-particle wave functions [45]. Recently, our research delved into the fascinating phenomenon of quantized torque on a quantum emitter positioned in a double-V configuration. This intriguing effect arises from the quantum interference of spontaneous emission channels. Furthermore, we explored a scenario in which the interference in spontaneous emission could be modified by situating the emitter above the surface of a bismuth chalcogenide material while parallel vortex beams propagate [49].

Exploring the characteristics of the induced torque resulting from the interaction of light with various atom–light coupling schemes serves as a significant motivation for many researchers, mainly because of its potential applications. In particular, understanding the imparted torque on atoms is crucial for accurately characterizing the dynamics of an ensemble, and has the potential to be utilized in the development of superconducting atomic devices. Moreover, the induced torque can be harnessed to generate superflow and superposition of macroscopic states in atomic vapors, as demonstrated by Kapale et al. in their research [50]. Additionally, the use of quantum repeaters for transmitting flying qubits carrying an OAM has emerged as another application of the induced torque in recent studies, as cited by Alois et al. [51].

The focus of this study centers around the coherent manipulation of light-induced torque and the production of current flow in trapped media that have been coherently prepared. This system, known as the phaseonium medium, has been extensively used for various purposes, including the creation of matched pulses, the enhancement of the index of refraction, and the enhancement of nonlinear frequency conversion. Moreover, it has been employed for enhanced nonlinear optics, as demonstrated by Paspalakis et al. [52]. Recent studies have also explored the exchange of optical vortices between different frequencies in coherently prepared atomic media [53,54]. One prominent method to create such a coherent superposition of the multi-ground-states is involved in CPT technique [12–15], which has been widely used for preparing coherent superpositions in atomic ensembles. CPT relies on a combination of laser fields, carefully tuned to drive transitions between the atomic ground states, leading to a coherent superposition of these states. By precisely controlling the laser parameters, such as frequency and intensity, one can achieve the desired coherent state preparation. Another approach involves the use of a transverse magnetic field, which can couple the atomic ground states and establish the coherent superposition. Additionally, fractional or partial STIRAP [8] is another viable technique for generating coherent superpositions. In STIRAP, only a controlled fraction of the atomic population is transferred to the target state, resulting in a coherent superposition of the multi-ground states. Furthermore, the feasibility of producing a quantum superposition of metastable states from a single initial state in a tripod atom–light coupling scheme has been demonstrated using a sequence of three pulses [55]. In experimental implementations, the choice of the most suitable method depends on the specific atomic species and the level structure of the system under investigation. Researchers carefully design the experimental setup and laser configurations to achieve efficient and precise coherent state preparation.

In this investigation, we explore the interaction of optical vortices carrying OAM with coherently prepared media. Initially, we examine the case of Λ atoms and later generalize the model to include the tripod and multi-level atom–light coupling schemes, utilizing additional laser beams. In this model, we assume that the atoms are prepared in a coherent superposition of lower levels and are interacting with weak probe fields, resulting in a CPT medium. This is different from traditional EIT schemes with a weak probe and a strong control. Our study provides the fundamental equations that describe the quantized torque imposed by optical vortices on the center of mass of each multilevel atom. This torque can rotate the ensemble about the beam axis, thereby creating an atomic current in the form of a ring. Notably, in comparison to previous approaches, the induced torque is strongly influenced by the initial internal state of the atoms. This factor provides a new degree of freedom for manipulating the torque and resulting current flow.

To observe such an induced torque in a real experiment, several steps are required. First, the atomic ensemble needs to be prepared in a coherent superposition of lower levels. This preparation ensures that the atoms are in the desired state to interact with the optical vortices. The next step involves generating optical vortices, which are beams carrying quantized OAM. These can be created using holographic techniques, spatial light modulators, or mode converters. Precise control over the topological charge of the vortices is crucial as it directly influences the quantized torque experienced by the trapped atoms. The prepared atomic ensemble is then allowed to interact with the optical vortices using a carefully designed experimental setup, ensuring proper alignment and overlap between the atomic ensemble and the vortex beams. To observe the predicted light-induced torque, one can employ sensitive

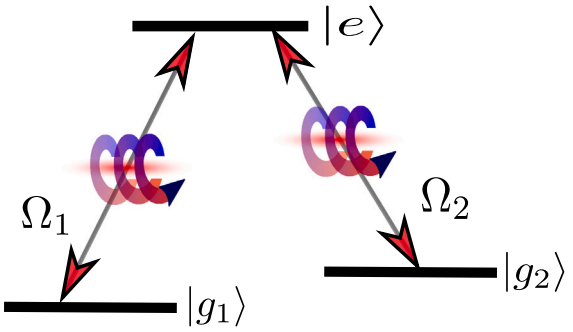

Fig. 1. Schematic diagram of the Λ atoms interacting with optical vortices.

techniques to measure the rotation of the trapped atoms caused by the interaction with the vortex beams, involving monitoring the collective motion of the atomic ensemble or using atom interferometry techniques to detect the phase shift induced by the torque. By systematically varying the initial internal state of the atoms and the strength of the vortex pair, one can explore the control parameters that influence the magnitude of the torque and current flow.

2. Case of Λ atom

In this work, we begin by examining a Λ-type atomic configuration, illustrated in Fig. 1, in which an excited state $|e\rangle$ is coupled to two lower states $|g_1\rangle$ and $|g_2\rangle$ via laser fields Ω_1 and Ω_2. Using cylindrical coordinates to describe the center-of-mass position vector of the atom, $\mathbf{R} = (r, \phi, z)$, we can express the atom–light Hamiltonian in the appropriate rotating frame and interaction picture as

$$H_\Lambda = \Omega_1|g_1\rangle\langle e| + \Omega_2|g_2\rangle\langle e| + \text{H.c.}. \tag{1}$$

The evolution of the pulse pair Ω_1 and Ω_2 and the atomic coherences ρ_{g_1e} and ρ_{g_2e} are described by the optical Bloch equations (OBEs):

$$\dot{\rho}_{g_1e} = i(\delta_1 + i\gamma_{eg_1})\rho_{g_1e} - i\Omega_1(\rho_{ee} - \rho_{g_1g_1}) + i\Omega_2\rho_{g_1g_2}, \tag{2}$$

$$\dot{\rho}_{g_2e} = i\left(\delta_2 + i\gamma_{eg_2}\right)\rho_{g_2e} - i\Omega_2(\rho_{ee} - \rho_{g_2g_2}) + i\Omega_1\rho_{g_2g_1}. \tag{3}$$

The detunings of the laser beams are defined as $\delta_1 = \omega_{eg_1} - \omega_1$ and $\delta_2 = \omega_{eg_2} - \omega_2$, where ω_{eg_1}, ω_{eg_2}, ω_1, and ω_2 are the frequencies of the transitions $|g_1\rangle \leftrightarrow |e\rangle$ and $|g_2\rangle \leftrightarrow |e\rangle$, as well as the central frequencies of the laser beams, respectively. The rates of decay from the excited state $|e\rangle$ to the lower states $|g_1\rangle$ and $|g_2\rangle$ are γ_{eg_1} and γ_{eg_2}, respectively. It is essential to note that these decay rates encompass both the spontaneous decay rate and the dephasing rate. Yet, since we assume $\gamma_{eg_1} = \gamma_{eg_2} = \gamma$ and scale all the involving parameters by γ, the specific values of the individual decay rates γ_{eg_1} and γ_{eg_2} do not affect our main results. As a result, any distinction in these decay rates would have already been incorporated into the scaled parameter γ.

We assume that the Λ atoms are prepared in a coherent superposition of both lower energy levels at the initial time, as represented by the following wave function:

$$|\psi(0)\rangle = c_1|g_1\rangle + c_2|g_2\rangle. \tag{4}$$

Here, c_1 and c_2 are the initial probability amplitudes associated with the two energy levels. In addition, we assume that the atom–light coupling is weak, satisfying the condition $|\Omega_1|, |\Omega_2| \ll \gamma_{eg_1}, \gamma_{eg_2}$. Under this approximation, we can obtain the first-order approximations for the density matrix elements as follows: $\rho_{ee} \approx 0$, $\rho_{g_1g_1} \approx |c_1|^2$, $\rho_{g_2g_2} \approx |c_2|^2$, and $\rho_{g_1g_2} \approx c_1c_2^*$. It should be pointed out that the population of the excited level, ρ_{ee}, is obtained as a second-order term. Consequently, in the first-order approximation ($\rho_{ee} \approx 0$), this term becomes negligible as we neglect second-order and higher terms. These higher-order terms have smaller contributions in the regime under study. Conversely, the atomic coherence between the ground state and the excited states (ρ_{eg_1}, ρ_{eg_2}) represents first-order terms in the Rabi frequency and, as such, remain non-zero in the first-order approximation [53,56]. Given these approximations, the steady-state solutions for the coherences ρ_{g_1e} and ρ_{g_2e} are given by:

$$\rho_{g_1e} = -\frac{|c_1|^2\Omega_1 + c_1c_2^*\Omega_2}{\delta_1 + i\gamma_{eg_1}}, \tag{5}$$

$$\rho_{g_2e} = -\frac{c_1^*c_2\Omega_1 + |c_2|^2\Omega_2}{\delta_2 + i\gamma_{eg_2}}, \tag{6}$$

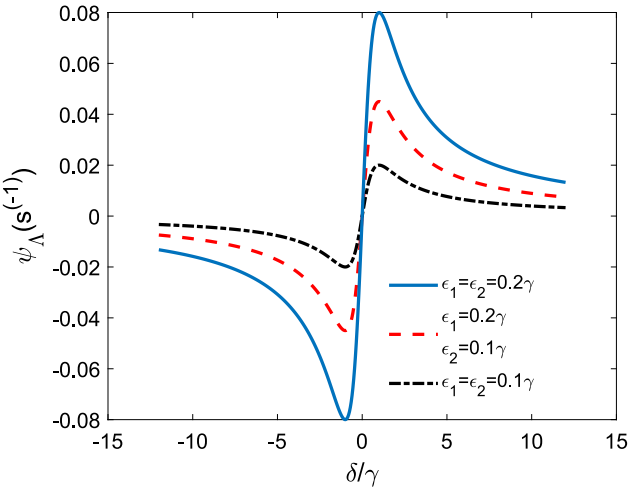

Fig. 2. Dependence of the torque function ψ_Λ (in units of s^{-1}) on the detuning parameter δ (in units of γ where $\gamma_{eg_1} = \gamma_{eg_2} = \gamma$) for different strengths of the vortex beams, when $|c_1|^2 = |c_2|^2 = 1/2$.

where δ_1 and δ_2 are the detunings of the two laser fields from the respective atomic transitions. It is important to note that the first-order approximation is valid only when $|\rho_{g_1e}|, |\rho_{g_2e}| \ll 1$. If this condition is not satisfied, we cannot assume that $\rho_{g_1g_1}$ and $\rho_{g_1g_2}$ are not changing during propagation.

In our analysis, we approach incident beams Ω_1 and Ω_2 as optical vortices characterized by unique properties:

$$\Omega_1 = |\Omega_1| e^{i\theta_1(\mathbf{R})}, \tag{7}$$

$$\Omega_2 = |\Omega_2| e^{il\theta_2(\mathbf{R})}, \tag{8}$$

Here, $|\Omega_1|$ and $|\Omega_2|$ signify the Rabi frequencies of the respective beams, while $\theta_1(\mathbf{R})$ and $\theta_2(\mathbf{R})$ represent the phase functions associated with the optical fields. These properties render the beams distinct and enable us to explore their diverse characteristics. Given the assumption of a many-body wave function of trapped atoms approximated as a product of identical single-atom wave functions, each atom experiences an identical force due to the incident light. The single-atom wave function can be factored into internal and center-of-mass wave functions. As a result, the force acting on the center-of-mass coordinate $\mathbf{R}$ is solely dependent on the density matrix elements of the internal states [48] and can be obtained using the OBEs from (2)–(3).

By factoring the single-atom wave function in this manner, we can find the scattering force F_Λ experienced by the Λ atom. This force can be expressed as

$$F_\Lambda = 2\hbar \left[\nabla\theta_1(\mathbf{R}) |\Omega_1| (\rho_{eg_1} + \rho_{g_1e}) + \nabla\theta_2(\mathbf{R}) |\Omega_2| (\rho_{eg_2} + \rho_{g_2e}) \right], \tag{9}$$

where ρ_{g_1e} and ρ_{g_2e} are the atomic coherences described in Eqs. (5)–(6). This expression reveals how the optical vortices in the incident beams generate a force that depends on the atomic coherences of the internal states, providing insight into the unique dynamics of the trapped atoms.

The doughnut Laguerre–Gaussian (LG) beams are characterized by a unique spatial distribution, given by the following expressions:

$$|\Omega_1| = \epsilon_1 \left(\frac{r}{w}\right)^{|l|} e^{-r^2/w^2}, \tag{10}$$

$$|\Omega_2| = \epsilon_2 \left(\frac{r}{w}\right)^{|l|} e^{-r^2/w^2}, \tag{11}$$

where r represents the cylindrical radius, l is the orbital angular momentum (OAM) number, ϕ denotes the azimuthal angle, w is the beam waist, and ϵ_1 and ϵ_2 represent the strength of the vortex beams. It is important to note that the effects of interest occur near the beam waist situated in the plane $z = 0$.

The angular dependence of the beams is described by

$$\theta_1(\mathbf{R}) = \theta_2(\mathbf{R}) = -l\phi. \tag{12}$$

Using Eq. (9) for the force, we can express it as

$$\begin{aligned} F_\Lambda =& 2\hbar \left[\nabla\theta_1 |\Omega_1| (\rho_{eg_1} + \rho_{g_1e}) + \nabla\theta_2 |\Omega_2| (\rho_{eg_2} + \rho_{g_2e}) \right] \\ =& 2\hbar k Y_\Lambda \left(\frac{r}{w}\right)^{2|l|} e^{-2r^2/w^2} \hat{z} + \frac{2\hbar l}{r} \psi_\Lambda \left(\frac{r}{w}\right)^{2|l|} e^{-2r^2/w^2} \hat{\phi}, \end{aligned} \tag{13}$$

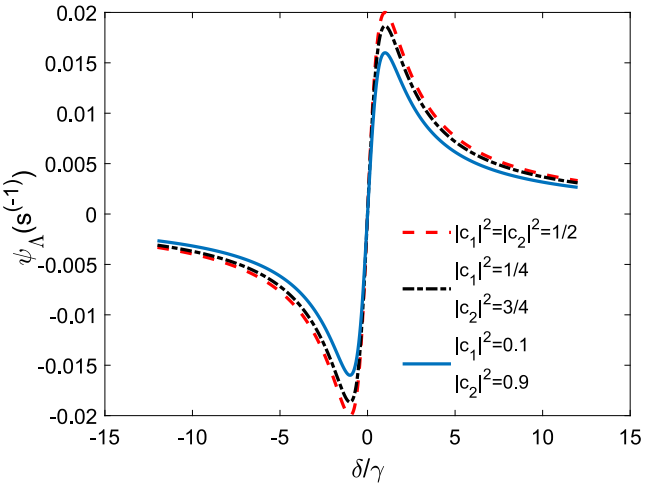

Fig. 3. Dependence of the torque function ψ_Λ (in units of s^{-1}) on the detuning parameter δ (in units of γ where $\gamma_{eg_1} = \gamma_{eg_2} = \gamma$) for different values of initial internal state coefficients c_i, when $\epsilon_1 = \epsilon_2 = 0.1\gamma$.

where

$$Y_\Lambda = \epsilon_1(\rho_{eg_1} + \rho_{g_1e}) - \epsilon_2(\rho_{eg_2} + \rho_{g_2e}), \tag{14}$$

$$\psi_\Lambda = -\left(\epsilon_1(\rho_{eg_1} + \rho_{g_1e}) + \epsilon_2(\rho_{eg_2} + \rho_{g_2e})\right). \tag{15}$$

The torque that is generated on the atoms' center of mass around the beam axis can be expressed as:

$$T_\Lambda = r \times F_\Lambda = 2\hbar l \psi_\Lambda \left(\frac{r}{w}\right)^{2|l|} e^{-2r^2/w^2} \hat{z}. \tag{16}$$

Figs. 2 and 3 illustrate the evolution of the function ψ_Λ in the torque equation (Eq. (15)). Our findings reveal that this function exhibits a dispersion behavior, with a maximum value occurring around $\delta = \pm\gamma$ and always being zero at line center $\delta = 0$. By manipulating the strengths of the vortex beams, the maximum value of ψ_Λ at $\delta = \pm\gamma$ can be increased. Fig. 3 further demonstrates that the function ψ_Λ and, consequently, the torque can be affected out of resonance by manipulating the population of the lower superposition states, as evidenced by the variation of ψ_Λ with respect to δ for different initial internal state coefficients c_i. These results highlight the significant impact of beam strength and population manipulation on the torque generated on the center of mass of Λ atoms around the beam axis.

It is important to note that the induced torque on the center of mass of Λ atoms, as described by Eq. (16), is quantized. The torque function is dependent on the OAM number l and the radial position, and as shown in Fig. 4, the intensity of the induced torque increases with increasing l. The figure also highlights the existence of a region of maximum intensity, which creates an optical dipole potential trap that attracts the atoms. In this region, the torque is also at its maximum, which results in the generation of a doughnut-shaped atomic flow. These findings underscore the potential of this approach for creating and manipulating atomic flow patterns using optical vortex beams.

3. Case of tripod and multi-level atoms

Let us now delve into the intricacies of how three light pulses interact with a four-level atom in the tripod configuration, as depicted in Fig. 5. In this configuration, the excited state $|e\rangle$ is coupled to three lower levels, namely $|g_1\rangle$, $|g_2\rangle$, and $|g_3\rangle$, through three distinct laser pulses denoted by Ω_1, Ω_2, and Ω_3, respectively. By switching to the interaction representation, the corresponding Hamiltonian for the tripod scheme can be expressed as:

$$H_T = \Omega_1|g_1\rangle\langle e| + \Omega_2|g_2\rangle\langle e| + \Omega_3|g_3\rangle\langle e| + \text{H.c.},. \tag{17}$$

The dynamics of the atom can be described using the equations of motion, which can be derived from the Hamiltonian of the system. In the case of the tripod configuration, the atomic equations of motion reads

$$\dot{\rho}_{g_1e} = i(\delta_1 + i\gamma_{eg_1})\rho_{g_1e} - i\Omega_1(\rho_{ee} - \rho_{g_1g_1}) + i\Omega_2\rho_{g_1g_2} + i\Omega_3\rho_{g_1g_3}, \tag{18}$$

$$\dot{\rho}_{g_2e} = i\left(\delta_1 + i\gamma_{eg_2}\right)\rho_{g_2e} - i\Omega_2(\rho_{ee} - \rho_{g_2g_2}) + i\Omega_1\rho_{g_2g_1} + i\Omega_3\rho_{g_2g_3}, \tag{19}$$

$$\dot{\rho}_{g_3e} = i\left(\delta_1 + i\gamma_{eg_3}\right)\rho_{g_3e} - i\Omega_3(\rho_{ee} - \rho_{g_3g_3}) + i\Omega_1\rho_{g_3g_1} + i\Omega_2\rho_{g_3g_2}. \tag{20}$$

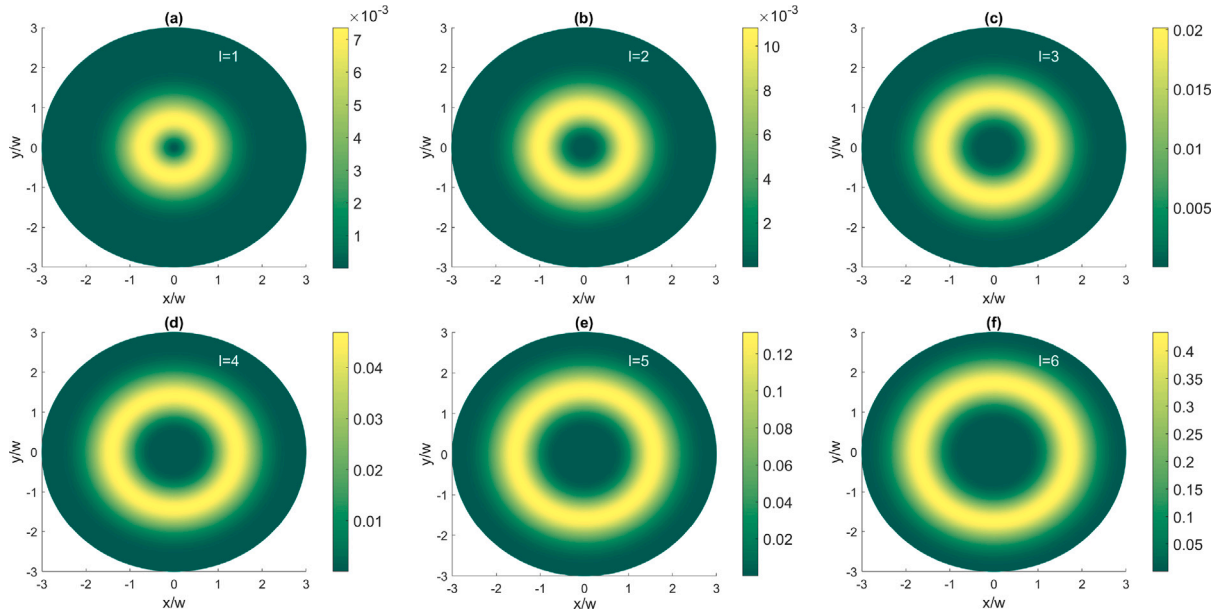

Fig. 4. (a)–(f) The ring shaped atomic flow generated for the trapped Λ atoms after experiencing a torque given by Eq. (16) and for different OAM numbers $l = 1 - 6$. Here, $|c_1|^2 = |c_2|^2 = 1/2$, $\epsilon_1 = \epsilon_2 = 0.1\gamma$, $\delta = \gamma$.

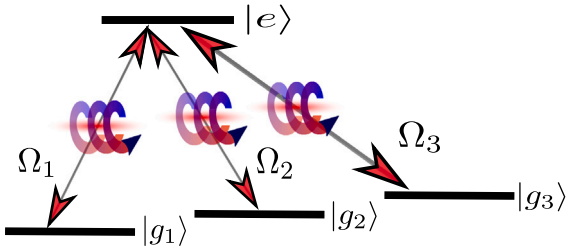

Fig. 5. Schematic diagram of the tripod atoms interacting with optical vortices.

Assuming that the tripod atoms are initially prepared in a superposition state given by

$$|\psi(0)\rangle = c_1|g_1\rangle + c_2|g_2\rangle + c_3|g_3\rangle, \tag{21}$$

and considering a sufficiently weak atom–light interaction such that $|\Omega_j| \ll \gamma_{eg_j}$, where γ_{eg_j} represents the decay rate of the $|e\rangle \rightarrow |g_j\rangle$ transition, we can approximate the density matrix elements as follows: $\rho_{ee} \approx 0$, $\rho_{g_1g_1} \approx |c_1|^2$, $\rho_{g_2g_2} \approx |c_2|^2$, $\rho_{g_3g_3} \approx |c_3|^2$, $\rho_{g_1g_2} \approx c_1c_2$, $\rho_{g_1g_3} \approx c_1c_3$, and $\rho_{g_2g_3} \approx c_2c_3^*$.

Under these conditions, we obtain a set of steady-state equations for the atomic coherences as

$$\rho_{g_1e} = -\frac{|c_1|^2\Omega_1 + c_1c_2^*\Omega_2 + c_1c_3^*\Omega_3}{\delta_1 + i\gamma_{eg_1}}, \tag{22}$$

$$\rho_{g_2e} = -\frac{c_1^*c_2\Omega_1 + |c_2|^2\Omega_2 + c_2c_3^*\Omega_3}{\delta_2 + i\gamma_{eg_2}}, \tag{23}$$

$$\rho_{g_3e} = -\frac{c_1^*c_3\Omega_1 + c_2^*c_3\Omega_2 + |c_3|^2\Omega_3}{\delta_3 + i\gamma_{eg_3}}. \tag{24}$$

The incident optical vortices are characterized by

$$\Omega_1 = |\Omega_1|e^{il\theta_1(\mathbf{R})}, \tag{25}$$

$$\Omega_2 = |\Omega_2|e^{il\theta_2(\mathbf{R})}, \tag{26}$$

$$\Omega_3 = |\Omega_3|e^{il\theta_3(\mathbf{R})}, \tag{27}$$

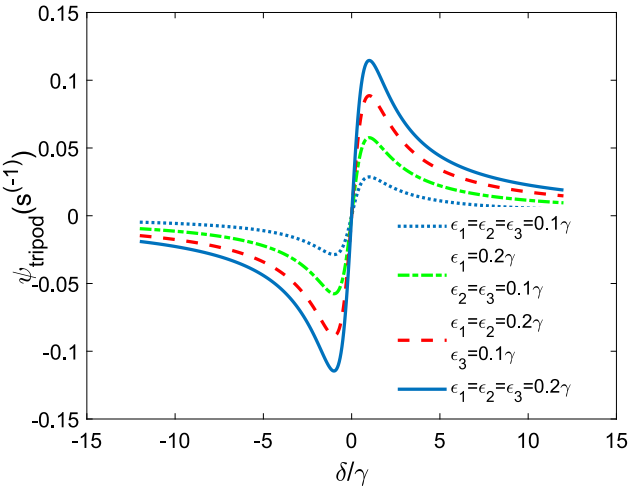

Fig. 6. Dependence of the torque function ψ_A (in units of s^{-1}) on the detuning parameter δ (in units of γ where $\gamma_{eg_1} = \gamma_{eg_2} = \gamma_{eg_3} = \gamma$) for different strengths of the vortex beams, when $|c_1|^2 = 1/2$, $|c_2|^2 = 1/3$, $|c_3|^2 = 1/6$.

where

$$|\Omega_1| = \epsilon_1 (\frac{r}{w})^{|l|} e^{-r^2/w^2}, \tag{28}$$

$$|\Omega_2| = \epsilon_2 (\frac{r}{w})^{|l|} e^{-r^2/w^2}, \tag{29}$$

$$|\Omega_3| = \epsilon_3 (\frac{r}{w})^{|l|} e^{-r^2/w^2}, \tag{30}$$

and

$$\theta_1(\mathbf{R}) = \theta_2(\mathbf{R}) = \theta_3(\mathbf{R}) = -l\phi. \tag{31}$$

The scattering force F_{tripod} for the tripod system changes to

$$F_{tripod} = 2\hbar \left[\nabla\theta_1 |\Omega_1| (\rho_{eg_1} + \rho_{g_1 e}) + \nabla\theta_2 |\Omega_2| (\rho_{eg_2} + \rho_{g_2 e}) + \nabla\theta_3 |\Omega_3| (\rho_{eg_3} + \rho_{g_3 e})\right] \tag{32}$$

where ρ_{eg_1}, ρ_{eg_2} and ρ_{eg_3} are given by Eqs. (22)–(24).

The induced torque about the beam axis for the tripod atom emerges as

$$T_{tripod} = r \times F_{tripod} = 2\hbar l \psi_{tripod} (\frac{r}{w})^{2|l|} e^{-2r^2/w^2} \hat{z}, \tag{33}$$

where

$$\psi_{tripod} = -\left(\epsilon_1 (\rho_{eg_1} + \rho_{g_1 e}) + \epsilon_2 (\rho_{eg_2} + \rho_{g_2 e}) + \epsilon_3 (\rho_{eg_3} + \rho_{g_3 e})\right). \tag{34}$$

The function ψ_{tripod} in the torque equation Eq. (33) for the tripod atoms varies as shown in Figs. 6 and 7. These figures illustrate the effect of the initial population distributions and the incident optical vortices intensities on the induced torque. Figure 8 shows the atomic flow in the shape of a ring generated for the trapped tripod atoms. It can be seen that the induced torque, in this case, is much larger than the case of the three-level Λ scheme described in the previous section (see Figs. 6–8). We can now generalize the above-described model of light-induced torque and persistent current flow by considering a system of n-component light pulses interacting with $(n+1)$-state atoms, where n lower atomic states $|g_1\rangle$, $|g_2\rangle$, …, $|g_n\rangle$ and one excited state $|e\rangle$ are present (Fig. 9). The interaction Hamiltonian for this multi-level atom system can be expressed as

$$H_{\mathrm{M}} = \sum_{m=1}^{n} \Omega_m |g_m\rangle\langle e| + \mathrm{H.c.}, \tag{35}$$

The dynamics of the density matrix ρ for the $n+1$-state atom system under the influence of the multi-component light pulses can be described by the following master equation

$$\dot{\rho}_{g_m e} = i(\delta_m + i\gamma_{eg_m})\rho_{g_m e} - i\Omega_m(\rho_{ee} - \rho_{g_m g_m}) + i \sum_{j=1; j\neq m}^{n} \Omega_j \rho_{g_m g_j}, \tag{36}$$

with $m = 1, 2, \ldots, n$.

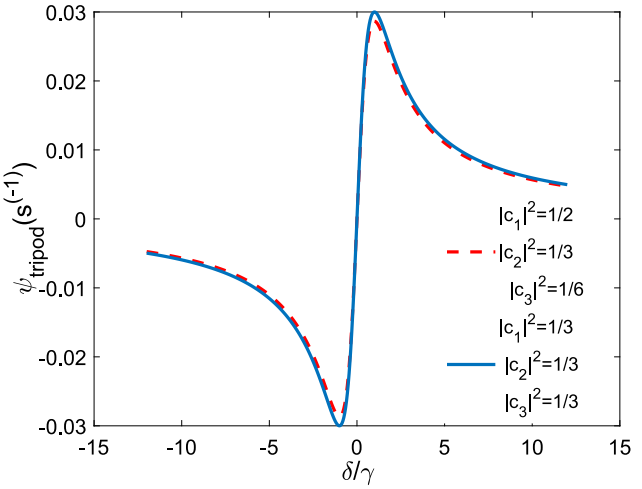

Fig. 7. Dependence of the torque function ψ_Λ (in units of s^{-1}) on the detuning parameter δ (in units of γ where $\gamma_{eg_1} = \gamma_{eg_2} = \gamma_{eg_3} = \gamma$) for different values of initial internal state coefficients c_i, when $\epsilon_1 = \epsilon_2 = \epsilon_3 = 0.1\gamma$.

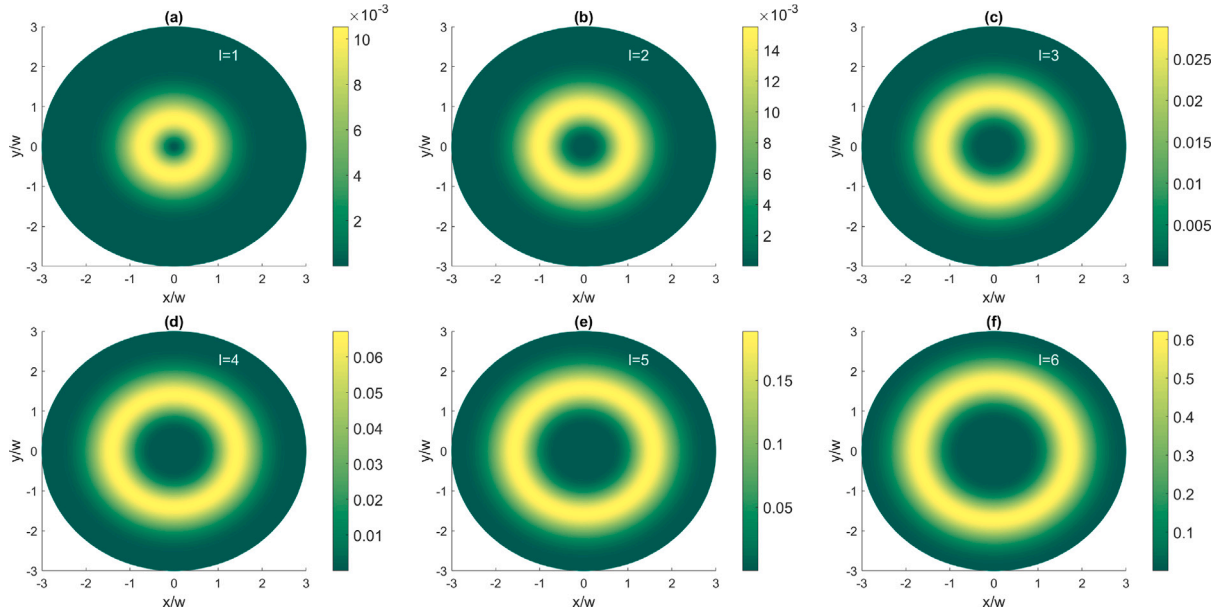

Fig. 8. (a)–(f) The ring atomic flow generated for the trapped tripod atoms after experiencing a torque given by Eq. (33) and for different OAM numbers $l = 1 - 6$. Here, $|c_1|^2 = 1/2$, $|c_2|^2 = 1/3$, $|c_3|^2 = 1/6$, $\epsilon_1 = \epsilon_2 = \epsilon_3 = 0.1\gamma$, $\delta = \gamma$.

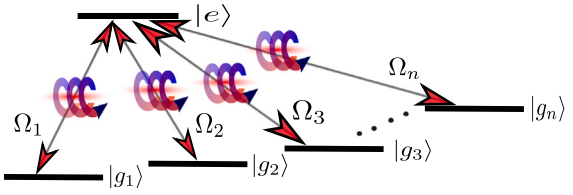

Fig. 9. Schematic diagram of the multi-level atom interacting with optical vortices.

The multi-level atoms are initially in the superposition state

$$|\psi(0)\rangle = \sum_{m=1}^{n} c_m |g_m\rangle. \tag{37}$$

For the weak atom–light interaction $|\Omega_j| \ll \gamma_{eg_j}$ and approximating $\rho_{ee} \approx 0$, $\rho_{g_m g_m} \approx |c_m|^2$ and $\rho_{g_m g_{m'}} \approx c_m c_{m'}^*$, $(m, m' = 1, 2, \ldots, n)$ to the first order in all laser fields, yields

$$\rho_{g_m e} = -\frac{\sum_{j=1}^{n} c_m c_j^* \Omega_j}{\delta_m + i\gamma_{eg_m}}, \ m = 1, 2, \ldots, n \tag{38}$$

where

$$\Omega_m = \varepsilon_m e^{il\theta_m(\mathbf{R})}, \tag{39}$$

are the multi-component vortices, and

$$|\Omega_m| = \varepsilon_m \left(\frac{r}{w}\right)^{|l|} e^{-r^2/w^2}, \tag{40}$$

$$\theta_1(\mathbf{R}) = \theta_2(\mathbf{R}) = \cdots = \theta_n(\mathbf{R}) = -l\phi. \tag{41}$$

The multi-level atom scattering force F_M becomes

$$F_M = 2\hbar \left[\sum_{j=1}^{n} \nabla\theta_j |\Omega_j| (\rho_{eg_j} + \rho_{g_j e})\right], \tag{42}$$

giving the induced torque in a general form

$$T_M = r \times F_M = 2\hbar l \psi_M \left(\frac{r}{w}\right)^{2|l|} e^{-2r^2/w^2} \hat{z}, \tag{43}$$

where

$$\psi_M = -\left(\sum_{j=1}^{n} \epsilon_j (\rho_{eg_j} + \rho_{g_j e})\right). \tag{44}$$

Clearly, adding additional atomic levels and laser fields can indeed increase the controllability over the induced torque. Indeed, in a multi-level atom system, the scattering force and induced torque are determined by the complex interplay between the laser fields and atomic energy levels. By adding more atomic levels and laser fields, it is possible to create a more complex energy level structure and to control the interactions between them more precisely. This allows for greater flexibility in designing the laser field parameters, such as their intensity, frequency, and polarization, to manipulate the scattering force and induced torque. Furthermore, adding more atomic levels can also increase the sensitivity of the system to changes in the laser field parameters, which can be useful for sensing applications. For example, the induced torque in a multi-level atom system can be used as a sensitive probe for measuring small forces or rotations.

Implementing a Λ (tripod) level scheme with two (or three) ground states and one excited state is a promising experimental setup, and one approach to realize it is by utilizing ^{87}Rb atoms. In this scheme, the excited level denoted as $|e\rangle$ can be associated with the $|5P_{1/2}, F = 1, m_F = 0\rangle$ state. The lower states, namely $|g_1\rangle$ and $|g_2\rangle$ (and possibly $|g_3\rangle$), can be identified as $|5S_{1/2}, F = 1, m_F = 1\rangle$ and $|5S_{1/2}, F = 1, m_F = -1\rangle$ (and potentially $|5S_{1/2}, F = 2, m_F = 0\rangle$) [53]. The Λ, tripod, or multi-level schemes provide a versatile platform for studying quantum coherence and interference phenomena. The two, three, or more ground states, with their distinct characteristics, allow for exploring interesting phenomena like dark-state polaritons and multi-color EIT. These effects are crucial for developing efficient quantum memories and quantum-enhanced sensing devices. The choice of ^{87}Rb atoms for this scheme is well-founded due to their desirable properties, including long coherence times and relatively easy manipulation through laser cooling and trapping techniques. Moreover, the $|5S_{1/2}, F = 1\rangle \rightarrow |5P_{1/2}, F = 1\rangle$ transition in rubidium is well studied, making it easier to control and measure the dynamics of the system accurately.

4. Concluding remarks

To summarize, this study has demonstrated that coherently prepared Λ-type multi-level atoms experience a persistent current flow when interacting with optical vortices. The atoms are initially prepared in a coherent superposition of the lower levels, and the atom–light coupling is assumed to be weak. The equations describing the quantized torque imposed by vortex beams on the center of mass of each trapped atom have been derived, and it has been shown that the induced torque is quantized and rotates the medium about the beam axis, creating a persistent atomic current in the form of a ring.

The study also highlights that the induced torque can be controlled and enhanced by the initial internal state of the atoms as well as the strength of the vortex beams. Furthermore, the model has been extended to more complicated schemes, such as the tripod and more complex level schemes involving additional laser pulses and atomic levels. This allows for greater control over the current flow and enhancement of the light-induced torque. Overall, this study provides insights into the behavior of multi-level atoms in the presence of optical vortices and demonstrates the potential for using such systems for precision control and manipulation of atomic currents.

Declaration of competing interest

The authors declare that they have no known competing financial interests or personal relationships that could have appeared to influence the work reported in this paper.

Data availability

Data will be made available on request.

References

[1] S.E. Harris, Electromagnetically induced transparency, Phys. Today 50 (1997) 36.
[2] Y. Wu, X. Yang, Electromagnetically induced transparency in υ-, Λ-, and cascade-type schemes beyond steady-state analysis, Phys. Rev. A 71 (2005) 053806.
[3] M.D. Lukin, Colloquium: Trapping and manipulating photon states in atomic ensembles, Rev. Modern Phys. 75 (2003) 457–472.
[4] M. Fleischhauer, A. Imamoglu, J.P. Marangos, Electromagnetically induced transparency: Optics in coherent media, Rev. Modern Phys. 77 (2005) 633–673.
[5] A. Kasapi, M. Jain, G.Y. Yin, S.E. Harris, Electromagnetically induced transparency: Propagation dynamics, Phys. Rev. Lett. 74 (1995) 2447–2450.
[6] E. Paspalakis, P.L. Knight, Electromagnetically induced transparency and controlled group velocity in a multilevel system, Phys. Rev. A 66 (2002) 015802.
[7] K. Bergmann, H. Theuer, B.W. Shore, Coherent population transfer among quantum states of atoms and molecules, Rev. Modern Phys. 70 (1998) 1003–1025.
[8] N.V. Vitanov, A.A. Rangelov, B.W. Shore, K. Bergmann, Stimulated Raman adiabatic passage in physics, chemistry, and beyond, Rev. Modern Phys. 89 (2017) 015006.
[9] B.T. Torosov, N.V. Vitanov, Composite stimulated Raman adiabatic passage, Phys. Rev. A 87 (2013) 043418.
[10] Y. Zhu, Lasing without inversion in a closed three-level system, Phys. Rev. A 45 (1992) R6149–R6152.
[11] J. Mompart, R. Corbalan, Lasing without inversion, J. Opt. B: Quantum Semiclass. Opt 2 (2000) R7–R24.
[12] G. Alzetta, A. Gozzini, L. Moi, G. Orriols, An experimental method for the observation of r.f. transitions and laser beat resonances in oriented Na vapour, Nuovo Cimento B 36 (1976) 5–20.
[13] H.R. Gray, R.M. Whitley, C.R. Stroud, Coherent trapping of atomic populations, Opt. Lett. 3 (1978) 218–220.
[14] P.M. Radmore, P.L. Knight, Population trapping and dispersion in a three-level system, J. Phys. B: At. Mol. Phys. 15 (1982) 561.
[15] E. Arimondo, Coherent population trapping in laser spectroscopy, Progress Opt. 35 (1996) 257.
[16] G. Juzeliūnas, H.J. Carmichael, Systematic formulation of slow polaritons in atomic gases, Phys. Rev. A 65 (2002) 021601(R).
[17] G. Juzeliūnas, P. Öhberg, Slow light in degenerate Fermi gases, Phys. Rev. Lett. 93 (2004) 033602.
[18] J. Ruseckas, V. Kudriašov, G. Juzeliūnas, R.G. Unanyan, J. Otterbach, M. Fleischhauer, Photonic-band-gap properties for two-component slow light, Phys. Rev. A 83 (2011) 063811.
[19] S.E. Harris, J.E. Field, A. Imamoğlu, Nonlinear optical processes using electromagnetically induced transparency, Phys. Rev. Lett. 64 (1990) 1107–1110.
[20] L. Deng, M.G. Payne, W.R. Garrett, Nonlinear frequency conversion with short laser pulses and maximum atomic coherence, Phys. Rev. A 58 (1998) 707–712.
[21] H. Kang, Y. Zhu, Observation of large Kerr nonlinearity at low light intensities, Phys. Rev. Lett. 91 (2003) 093601.
[22] H.R. Hamedi, G. Juzeliūnas, Phase-sensitive Kerr nonlinearity for closed-loop quantum systems, Phys. Rev. A 91 (2015) 053823.
[23] A.S. Zibrov, A.B. Matsko, O. Kocharovskaya, Y.V. Rostovtsev, G.R. Welch, M.O. Scully, Transporting and time reversing light via atomic coherence, Phys. Rev. Lett. 88 (2002) 103601.
[24] D.A. Braje, V. Balić, G.Y. Yin, S.E. Harris, Low-light-level nonlinear optics with slow light, Phys. Rev. A 68 (2003) 041801.
[25] I. Thanopulos, E. Paspalakis, V. Yannopapas, Optical switching of electric charge transfer pathways in porphyrin: A light-controlled nanoscale current router, Nanotechnology 19 (2008) 445202.
[26] L. Allen, M.J. Padgett, M. Babiker, IV the orbital angular momentum of light, Progress Opt. 39 (1999) 291–372.
[27] L. Marrucci, C. Manzo, D. Paparo, Optical spin-to-orbital angular momentum conversion in inhomogeneous anisotropic media, Phys. Rev. Lett. 96 (2006) 163905.
[28] N.R. Heckenberg, R. McDuff, C.P. Smith, A.G. White, Generation of optical phase singularities by computer-generated holograms, Opt. Lett. 17 (1992) 221–223.
[29] I.G. Mariyenko, J. Strohaber, C.J.G.J. Uiterwaal, Creation of optical vortices in femtosecond pulses, Opt. Express 13 (2005) 7599–7608.
[30] S. Slussarenko, A. Murauski, T. Du, V. Chigrinov, L. Marrucci, E. Santamato, Tunable liquid crystal q-plates with arbitrary topological charge, Opt. Express 19 (2011) 4085–4090.
[31] J. Ruseckas, G. Juzeliūnas, P. Öhberg, S.M. Barnett, Polarization rotation of slow light with orbital angular momentum in ultracold atomic gases, Phys. Rev. A 76 (2007) 053822.
[32] F. Castellucci, T.W. Clark, A. Selyem, J. Wang, S. Franke-Arnold, Atomic compass: Detecting 3D magnetic field alignment with vector vortex light, Phys. Rev. Lett. 127 (2021) 233202.
[33] Q.-F. Chen, B.-S. Shi, Y.-S. Zhang, G.-C. Guo, Entanglement of the orbital angular momentum states of the photon pairs generated in a hot atomic ensemble, Phys. Rev. A 78 (2008) 053810.
[34] S.M. Lloyd, M. Babiker, J. Yuan, Interaction of electron vortices and optical vortices with matter and processes of orbital angular momentum exchange, Phys. Rev. A 86 (2012) 023816.
[35] J. Ruseckas, V. Kudriašov, I.A. Yu, G. Juzeliūnas, Transfer of orbital angular momentum of light using two-component slow light, Phys. Rev. A 87 (2013) 053840.
[36] N. Radwell, T.W. Clark, B. Piccirillo, S.M. Barnett, S. Franke-Arnold, Spatially dependent electromagnetically induced transparency, Phys. Rev. Lett. 114 (2015) 123603.
[37] V.E. Lembessis, J. Courtial, N. Radwell, A. Selyem, S. Franke-Arnold, O.M. Aldossary, M. Babiker, Graphene-like optical light field and its interaction with two-level atoms, Phys. Rev. A 92 (2015) 063833.
[38] H.R. Hamedi, V. Kudriasov, J. Ruseckas, G. Juzeliunas, Azimuthal modulation of electromagnetically induced transparency using structured light, Opt. Express 26 (2018) 28249–28262.
[39] H.R. Hamedi, J. Ruseckas, E. Paspalakis, G. Juzeliūnas, Off-axis optical vortices using double-Raman singlet and doublet light-matter schemes, Phys. Rev. A 101 (2020) 063828.
[40] V.E. Lembessis, D. Ellinas, M. Babiker, O. Al-Dossary, Atom vortex beams, Phys. Rev. A 89 (2014) 053616.
[41] J.W.R. Tabosa, D.V. Petrov, Optical pumping of orbital angular momentum of light in cold cesium atoms, Phys. Rev. Lett. 83 (1999) 4967–4970.
[42] H. He, M.E.J. Friese, N.R. Heckenberg, H. Rubinsztein-Dunlop, Direct observation of transfer of angular momentum to absorptive particles from a laser beam with a phase singularity, Phys. Rev. Lett. 75 (1995) 826–829.

[43] M.E.J. Friese, J. Enger, H. Rubinsztein-Dunlop, N.R. Heckenberg, Optical angular-momentum transfer to trapped absorbing particles, Phys. Rev. A 54 (1996) 1593–1596.
[44] V. Garcés-Chávez, D. McGloin, M.J. Padgett, W. Dultz, H. Schmitzer, K. Dholakia, Observation of the transfer of the local angular momentum density of a multiringed light beam to an optically trapped particle, Phys. Rev. Lett. 91 (2003) 093602.
[45] M.F. Andersen, C. Ryu, P. Cladé, V. Natarajan, A. Vaziri, K. Helmerson, W.D. Phillips, Quantized rotation of atoms from photons with orbital angular momentum, Phys. Rev. Lett. 97 (2006) 170406.
[46] C.M. Herne, K.M. Capuzzi, E. Sobel, R.T. Kropas, Rotation of large asymmetrical absorbing objects by Laguerre-Gauss beams, Opt. Lett. 40 (2015) 4026–4029.
[47] M. Babiker, W.L. Power, L. Allen, Light-induced torque on moving atoms, Phys. Rev. Lett. 73 (1994) 1239–1242.
[48] V.E. Lembessis, M. Babiker, Light-induced torque for the generation of persistent current flow in atomic gas Bose-Einstein condensates, Phys. Rev. A 82 (2010) 051402.
[49] H.R. Hamedi, J. Ruseckas, V. Yannopapas, D. Karaoulanis, E. Paspalakis, Light-induced enhanced torque on double-V-type quantum emitters via quantum interference in spontaneous emission, Opt. Laser Technol. 165 (2023) 109550.
[50] K.T. Kapale, J.P. Dowling, Vortex phase qubit: Generating arbitrary, counterrotating, coherent superpositions in Bose-Einstein condensates via optical angular momentum beams, Phys. Rev. Lett. 95 (2005) 173601.
[51] A. Mair, A. Vaziri, G. Weihs, A. Zeilinger, Entanglement of the orbital angular momentum states of photons, Nature 412 (2001) 313–316.
[52] E. Paspalakis, P.L. Knight, Transparency, slow light and enhanced nonlinear optics in a four-level scheme, J. Opt. B: Quantum Semiclass. Opt 4 (2002) S372.
[53] H.R. Hamedi, J. Ruseckas, E. Paspalakis, G. Juzeliūnas, Transfer of optical vortices in coherently prepared media, Phys. Rev. A 99 (2019) 033812.
[54] H.R. Hamedi, E. Paspalakis, G. Žlabys, G. Juzeliūnas, J. Ruseckas, Complete energy conversion between light beams carrying orbital angular momentum using coherent population trapping for a coherently driven double-Λ atom-light-coupling scheme, Phys. Rev. A 100 (2019) 023811.
[55] R.G. Unanyan, B.W. Shore, K. Bergmann, Laser-driven population transfer in four-level atoms: Consequences of non-Abelian geometrical adiabatic phase factors, Phys. Rev. A 59 (1999) 2910–2919.
[56] H.R. Hamedi, E. Paspalakis, G. Žlabys, G. Juzeliūnas, J. Ruseckas, Complete energy conversion between light beams carrying orbital angular momentum using coherent population trapping for a coherently driven double-Λ atom-light-coupling scheme, Phys. Rev. A 100 (2019) 023811.